Check for updates

LIMNOLOGY and OCEANOGRAPHY

ASLO

Limnol. Oceanogr. 9999, 2021, 1–15
© 2021 The Authors. *Limnology and Oceanography* published by Wiley Periodicals LLC on behalf of Association for the Sciences of Limnology and Oceanography.
doi: 10.1002/lno.11793

Distinguishing zooplankton fecal pellets as a component of the biological pump using compound-specific isotope analysis of amino acids

Shannon C. Doherty,[1] **Amy E. Maas**,[2] **Deborah K. Steinberg**,[3] **Brian N. Popp**,[4] **Hilary G. Close**[1*]

[1]Rosenstiel School of Marine and Atmospheric Science, University of Miami, Miami, Florida
[2]Bermuda Institute of Ocean Sciences, St. George's, Bermuda
[3]Virginia Institute of Marine Science, William & Mary, Gloucester Point, Virginia
[4]Department of Earth Sciences, University of Hawaii at Mānoa, Honolulu, Hawaii

Abstract

Zooplankton contribute a major component of the vertical flux of particulate organic matter to the ocean interior by packaging consumed food and waste into large, dense fecal pellets that sink quickly. Existing methods for quantifying the contribution of fecal pellets to particulate organic matter use either visual identification or lipid biomarkers, but these methods may exclude fecal material that is not morphologically distinct, or may include zooplankton carcasses in addition to fecal pellets. Based on results from seven pairs of wild-caught zooplankton and their fecal pellets, we assess the ability of compound-specific isotope analysis of amino acids (CSIA-AA) to chemically distinguish fecal pellets as an end-member material within particulate organic matter. Nitrogen CSIA-AA is an improvement on previous uses of bulk stable isotope ratios, which cannot distinguish between differences in baseline isotope ratios and fractionation due to metabolic processing. We suggest that the relative trophic position of zooplankton and their fecal pellets, as calculated using CSIA-AA, can provide a metric for estimating the dietary absorption efficiency of zooplankton. Using this metric, the zooplankton examined here had widely ranging dietary absorption efficiencies, where lower dietary absorption may equate to higher proportions of fecal packaging of undigested material. The nitrogen isotope ratios of threonine and alanine statistically distinguished the zooplankton fecal pellets from literature-derived examples of phytoplankton, zooplankton biomass, and microbially degraded organic matter. We suggest that $\delta^{15}N$ values of threonine and alanine could be used in mixing models to quantify the contribution of fecal pellets to particulate organic matter.

The biological pump comprises the fixation of carbon by phytoplankton in the surface ocean and subsequent physical removal of this fixed carbon from the surface to the ocean interior, largely by gravitational settling of particles (Longhurst and Glen Harrison 1989). Larger or denser particles have faster sinking velocities than smaller or less dense particles, and therefore may play an outsize role in carbon sequestration. In addition, small, suspended particles and large, sinking particles are often chemically distinct (Wakeham and Canuel 1988; Abramson et al. 2010). Zooplankton fecal pellets can influence both small and large particle chemistry through aggregation and disaggregation. By consuming phytoplankton and organic particles to produce compact, dense fecal pellets, zooplankton can package small, suspended particles to produce larger, more quickly settling particles (i.e., "biological aggregation," Lam and Marchal 2015). Zooplankton also leave chemical traces in smaller particles in the mesopelagic zone, indicating that material deriving from fecal pellets may also enter the suspended particle pool via disaggregation (Wakeham and Canuel 1988). The influence of fecal pellets on the biological pump is therefore dynamic, which necessitates measuring the contribution of fecal pellets to both particle pools to understand the role zooplankton play in the biological pump.

Current estimates of fecal pellet contribution to sinking particles vary with region, with values ranging widely from < 1% to 100% of carbon export across the global ocean (compilation by Turner, 2002, 2015). Zooplankton community ecology and water column characteristics (phytoplankton

*Correspondence: hclose@rsmas.miami.edu

This is an open access article under the terms of the Creative Commons Attribution-NonCommercial-NoDerivs License, which permits use and distribution in any medium, provided the original work is properly cited, the use is non-commercial and no modifications or adaptations are made.

Additional Supporting Information may be found in the online version of this article.

ecology, microbial activity, etc.) can influence the number, size, density, and sinking rate of fecal pellets (Dagg et al. 2014), contributing to these variable regional estimates. Previous studies rely on visual identification of fecal pellets caught in sediment traps (Wexels Riser et al. 2008; Atkinson et al. 2012); this method may, however, fail to capture fecal pellet material that is not morphologically distinct and potentially lead to an underestimation of fecal pellet contribution to particle export. A method that does not rely on visual identification also would be important in detecting the contribution of disaggregated fecal pellet to smaller particles in the suspended particle pools.

Fecal pellet contributions to carbon export are sometimes modeled rather than directly measured. Siegel et al. (2014) used a food web model to determine the contribution of fecal pellets to particle export out of the euphotic zone. In this study, fecal pellet flux was modeled as a fixed fraction of the grazing rate of zooplankton on phytoplankton, which allowed for an estimate of fecal pellet contribution to particle export that relied on experimentally determined rates and water column properties (e.g., net primary production, zooplankton community size). Other food web models (Michaels and Silver 1988) use a grazing rate-fixed assimilation efficiency to estimate how much organic matter passes through the food web into carbon export via fecal pellets. While a useful tool in predicting fecal pellet export, such models do not resolve the underlying particle dynamics and therefore cannot isolate the distribution of fecal pellet material through particle aggregation and disaggregation. They also rely on fixed rates and efficiencies, and while these are often consistent they can vary by organism and region (Steinberg and Landry 2017).

Lipid biomarkers are also sometimes used to estimate the contribution of zooplankton to particle production. However, most zooplankton biomarkers, such as wax esters, are compounds associated with zooplankton biomass (Wakeham and Canuel 1988; Pedrosa-Pàmies et al. 2018) and may not be proportionally present in their fecal pellets. Zooplankton biomass itself can, additionally, contribute to particles in the water column in the form of molts and carcasses (Steinberg and Landry 2017). For example, wax esters are primarily used by crustacean zooplankton for energy storage (Sargent and Falk-Petersen 1988; Lee et al. 2006), and therefore cannot be used to distinguish zooplankton biomass from fecal pellets, or identify fecal pellets of other types of zooplankton (e.g., gelatinous zooplankton). Cholesterol, another common zooplankton biomarker, is found in both fecal pellets and zooplankton (Harvey et al. 1989). Additionally, fecal pellets may chemically resemble the zooplankton diet, which may make fecal pellets indistinguishable from other particle components (Schnetzer and Steinberg 2002). Dinosterol, a biomarker for dinoflagellates, has been recovered in fecal pellets (Harvey et al. 1989). Lipid biomarkers therefore may have a limited use in distinguishing fecal pellets from zooplankton biomass or phytodetritus in particles.

Compound-specific isotope analysis of amino acids (CSIA-AA) is a promising tool for distinguishing the sources contributing to natural materials. Hannides et al. (2020), Gloeckler et al. (2018), and Romero-Romero et al. (2020) have used nitrogen CSIA-AA to determine the small vs. large particulate food sources forming the base of mesopelagic and bathypelagic food webs. Because nitrogen CSIA-AA records isotopic fractionation during metazoan and microbial metabolism (Chikaraishi et al. 2007; Ohkouchi et al. 2017), it may be able to track the metabolic alteration that occurs in fecal pellets, which distinguish them from other organic matter. Part of this distinction arises from the use of CSIA-AA to estimate the trophic position, or the level in the food web, of an organism (Chikaraishi et al. 2007). To our knowledge, the trophic position of fecal pellets has yet to be determined using this method. The trophic position of particles such as fecal pellets is imparted by the heterotrophic microbes that colonize them or the remnants of consumer biomass that they contain. Comparing zooplankton trophic position to corresponding fecal pellet trophic position could provide valuable information about the feeding strategies and dietary efficiencies of different species of zooplankton, or zooplankton communities in different oceanographic regions. In addition, while the carbon and nitrogen sources of fecal pellets may not differ from those of other organic matter in the environment, fecal pellets record a distinct metabolic history while in the gut.

Here, we characterize fecal pellets and corresponding zooplankton biomass from three ocean locations (Fig. 1) using both bulk and compound-specific isotope approaches to demonstrate that the CSIA-AA method records sufficient metabolic information to chemically distinguish fecal pellets as an organic matter end-member in the water column. We present here the first determination of zooplankton fecal pellet trophic position and compare CSIA-AA methods to bulk stable isotope methods. We suggest that the comparison of zooplankton biomass trophic position and fecal pellet trophic position can reflect relative assimilation efficiencies in zooplankton and therefore export potential of fecal pellet production, with a lower dietary assimilation efficiency corresponding to a higher export potential.

Methods

Zooplankton collection

Zooplankton were captured live on four cruises: one in the northeast Pacific near Ocean Station Papa (RR 1813, August 2018, Export Processes in the Ocean from Remote Sensing [EXPORTS]), two in the Sargasso Sea off Bermuda (AE 1819, July 2018 and AE 1910, May 2019; NSF OCE 1829318 and Bermuda Institute of Ocean Sciences-Simons Collaboration on Ocean Processes and Ecology [BIOS-SCOPE]), and one in the Southern Ocean off the western Antarctic Peninsula (LMG 1801, January 2018, Palmer Antarctica Long Term Ecological Research [PAL LTER]) (Table 1). Species collected in the

northeast Pacific were the salp *Salpa aspera* and amphipod *Vibilia propinqua*, Sargasso Sea collection included three size classes of combined mixed zooplankton community and one sampling of *Salpa* sp., and Antarctic krill *Euphausia superba* were collected in the Southern Ocean (Table 1). More detailed location information and collection methods for each cruise are included in Supplementary Table S1. Generally, a Reeve, Metro, or ring net was deployed at night in the upper 200 m to catch both resident and vertically migrating zooplankton. Upon recovery, contents of the cod end were diluted into a larger volume tub containing surface seawater. In the case of species-specific samples, animals were picked individually from the tub using a small container or ladle (for live experiments) or a fine mesh aquarium net. In the case of mixed communities, the cod end was gently filtered through different combinations of sieves submerged in filtered seawater to generate size-fractioned subsamples, similar to the approach of Stamieszkin et al. (2021); those analyzed here include > 1, 1–2.5, and 0.25–1 mm.

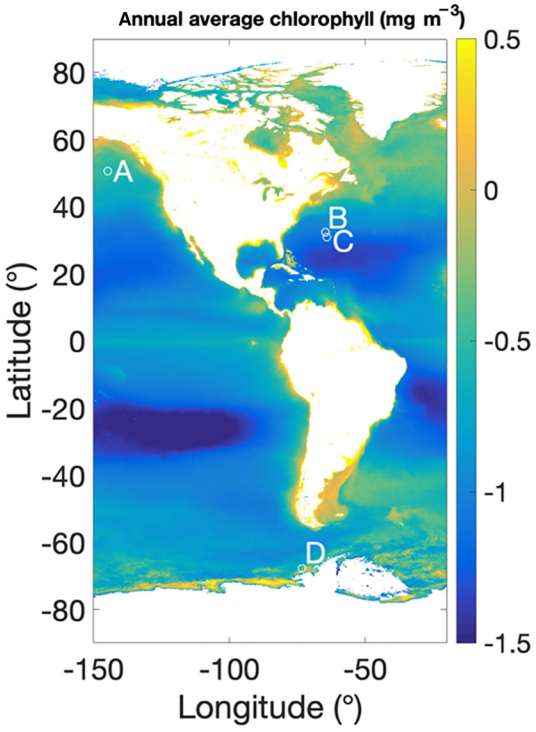

Fig. 1. Sample locations plotted over log of annual average surface chlorophyll (mg/m3). Data from Melin (2013). Locations of cruises: (**A**) RR 1813, (**B**) AE 1910, (**C**) AE 1819, and (**D**) LMG 1801.

Fecal pellet generation

After collection, animals were incubated in 0.2 μm filtered seawater. The incubation chambers consisted of two nested plastic containers: an intact exterior container, and an interior container with a mesh bottom of pore size smaller than the zooplankton, both acid-cleaned. The zooplankton swam freely in the filtered seawater above the mesh, and their fecal pellets fell through the mesh to the bottom of the exterior container. Incubation times were mostly 9–12 h in duration, with the exception of Sargasso Sea salps, which produced plentiful and visible fecal pellets in < 2 h (see Table S1). At the end of each incubation, animals were removed on the mesh of the interior container, rinsed with filtered seawater, and immediately stored in precombusted foil in a −80°C freezer. The remaining water from the experiment contained the fecal pellets and was filtered onto acid-cleaned 6 μm Nitex or precombusted 0.7 μm GF/F filters (Table S1). Filters were stored in precombusted foil at −80°C.

Sample preparation

With the exception of the *E. superba* samples, which partially thawed on transport and were refrozen, zooplankton and fecal pellet filters remained frozen at −80°C until processing in the lab. Once in the lab, zooplankton and fecal pellets collected onto Nitex mesh were rinsed onto precombusted glass fiber filters (GF/F) using filtered sea water (0.2 μm), returned to −80°C and lyophilized. Ten to 30 whole animals from each experiment were then homogenized with a mortar and pestle and stored in precombusted glass vials at room temperature in a desiccator until further preparation. Dried fecal pellet filters were checked for zooplankton and

Table 1. Details of zooplankton and fecal pellet samples including collection year, season, oceanographic region, species collected, and typical diet of collected species.

Cruise	Year	Region	Season	Species	Diet
RR 1813	2018	Northeast Pacific	Summer	*Salpa aspera*	Indiscriminate filter feeders (Henschke et al. 2016)
				Vibilia propinqua	Specific and obligate parasite of *Salpa aspera* (Madin and Harbison 1977)
AE 1819	2018	Sargasso Sea	Summer	*Salpa* sp.	Indiscriminate filter feeders
AE 1910	2019	Sargasso Sea	Spring	Mixed community (three sizes)	Filter feeders, indiscriminate and selective, carnivores, detritivores (Schnetzer and Steinberg 2002)
LMG 1801	2018	Southern Ocean	Summer	*Euphausia superba*	Phytoplankton and microzooplankton filter feeders (Atkinson et al. 2012)

plastic contamination under a dissecting microscope. All identified zooplankton biomass and plastic was removed and filters were then stored at −20°C.

Bulk isotope analysis

Bulk isotope ratios were determined from the homogenized zooplankton and fecal pellet filters using a Thermo Scientific Flash Smart coupled with a MAT 253 isotope ratio mass spectrometer with a Conflo IV interface. Isotope values are reported relative to atmospheric N_2 for nitrogen and Vienna Pee Dee Belemnite for carbon ($R_{standard}$).

Compound-specific isotope analysis

Zooplankton and fecal pellet filters were hydrolyzed to extract amino acids (20 h at 110°C, 6N hydrochloric acid), purified on cation exchange resin columns (50W-X8, 100–200 mesh) and derivatized to trifluoroacetyl/isopropyl esters for gas chromatography following the methods of Hannides et al. (2013). Two to 5 g of homogenized zooplankton and a quarter of a fecal pellet filter were used in each hydrolysis. The derivatized amino acids were analyzed for nitrogen isotopic composition on a Thermo Trace 1310 gas chromatograph with a BPX5 column (50 m × 0.32 mm, 1.0 μm film thickness) through a combined combustion/reduction interface (Thermo Isolink II, 1000°C) and liquid nitrogen cold trap, interfaced to a Thermo Conflo IV and MAT 253 isotope ratio mass spectrometer. Three injections were made for each sample where possible, with norleucine and aminoadipic acid with known $\delta^{15}N$ values as coinjection standards. For some samples, only one injection was obtained due to either low protein content (e.g., species with high chitin or salt biomass weight) or to amino acid loss during purification procedures; through identical treatment of amino acid standards, such losses were determined to affect quantities of amino acids and not their isotopic values. A standard solution of 14 amino acids with known $\delta^{15}N$ values was also analyzed with each set of three injections to track instrument performance, and to correct for instrument drift, including that due to oxidation state of the reactor (Hannides et al., 2013). Data from standards injected over the lifetime of the instrument were used to correct for relationships between measured $\delta^{15}N$ values and peak area on the instrument.

Calculations and statistical analysis

Trophic position (TP) was calculated using the $\delta^{15}N$ values of glutamic acid/glutamine (Glx) and phenylalanine (Phe) according to the formulation of (Chikaraishi et al. 2009):

$$TP = \left(\delta^{15}N_{Glx} - \delta^{15}N_{Phe} - 3.4\right)/7.6 + 1 \quad (1)$$

Calculation of propagated uncertainty for trophic position followed Jarman et al. (2017) and was determined using the standard deviation of β and trophic discrimination factor terms from Chikaraishi et al. (2009) and the standard deviation of Glx and Phe $\delta^{15}N$ values for the replicate injections of each sample. In some cases, sufficient material was only available for one injection; a conservative analytical uncertainty of 1‰ was estimated for any amino acid that was measured only once in a given sample (Table S2).

We compared various $\delta^{15}N$ values and trophic position (TP) between zooplankton and their fecal pellet (FP) products as captured in a single incubation experiment:

$$\Delta\delta^{15}N_{zoop-FP} = \delta^{15}N_{zooplankton} - \delta^{15}N_{FP} \quad (2)$$

$$\Delta TP_{zoop-FP} = TP_{zooplankton} - TP_{FP} \quad (3)$$

Phe is considered a "source" amino acid—one that retains its $\delta^{15}N$ value from its initial synthesis by primary producers (Popp et al. 2007; Chikaraishi et al. 2009; Décima et al. 2017). To account for the source nitrogen isotopic variability between studies and locations, for statistical comparisons all amino acid $\delta^{15}N$ values were normalized by subtracting the Phe $\delta^{15}N$ value for each sample (hereby referred to as "Phe-normalized").

Amino acid $\delta^{15}N$ values for other marine organic matter end-members were collected from previously published studies: zooplankton size classes (McClelland et al. 2003; Hannides et al. 2009, 2013, 2020; Romero-Romero et al. 2020), cultured phytoplankton (McCarthy et al. 2013), and high molecular weight dissolved organic matter and mesopelagic ultra-filtered particulate organic matter (Yamaguchi and McCarthy 2018). High molecular weight dissolved organic matter and mesopelagic ultra-filtered particulate organic matter are considered here to be end-members representing microbially degraded organic matter, based on the interpretation of Yamaguchi and McCarthy (2018). The data from this study and previous studies were organized into groups by end-member: fecal pellets ($n = 7$), zooplankton ($n = 56$), phytoplankton ($n = 11$), and microbially degraded organic matter ($n = 4$). A one-way ANOVA of end-member $\delta^{15}N$ values was run for each Phe-normalized amino acid that was measured in all studies (threonine, Thr; alanine, Ala; Glx; aspartic acid, Asp; valine, Val; proline, Pro; glycine, Gly; leucine, Leu; serine, Ser) as well as ΣV, a proposed indicator for microbial resynthesis of trophic amino acids (McCarthy et al. 2007), calculated here without isoleucine (Eq. 4 and 5, where Tr refers to the average of the five trophic amino acids used) due to unavailability of isoleucine data for some samples. A Tukey's honest significant difference test (Tukey HSD) was run for each amino acid that returned an ANOVA $p < 0.05$.

$$\delta^{15}NTr = \frac{1}{5} \times \left(\delta^{15}NAla + \delta^{15}NGlx + \delta^{15}NAsp + \delta^{15}NPro + \delta^{15}NLeu\right) \quad (4)$$

$$\Sigma V = \frac{1}{5} \times \left(\left|\delta^{15}NAla - \delta^{15}NTr\right| + \left|\delta^{15}NGlx - \delta^{15}NTr\right| + \left|\delta^{15}NAsp - \delta^{15}NTr\right| + \left|\delta^{15}NPro - \delta^{15}NTr\right| + \left|\delta^{15}NLeu - \delta^{15}NTr\right|\right)$$

Results

Bulk results: $\delta^{15}N$, $\delta^{13}C$, C : N

Bulk $\delta^{15}N$ values of zooplankton ranged from 0.3‰ to 6.3‰, varying across study sites (Table 2; Fig. 2A). fecal pellets generally had lower $\delta^{15}N$ values than zooplankton, similar to the results of Altabet and Small (1990). However, some fecal pellets had $\delta^{15}N$ values similar to or within the uncertainty range of zooplankton (Table 2; Fig. 2A). Most values for bulk $\Delta\delta^{15}N_{zoop\text{-}FP}$ fell between −0.5‰ and 2.9‰ (Table 2). The major exception to this pattern was the Sargasso Sea *Salpa* sp. sample, which had fecal pellets with a bulk $\delta^{15}N$ value 4.1‰ higher than the zooplankton tissue (i.e., the bulk $\Delta\delta^{15}N_{zoop\text{-}FP}$ was −4.1‰).

Bulk $\delta^{13}C$ values of zooplankton biomass ranged from −27.2‰ to −21.2‰, varying across study sites (Table 2; Fig. 2B). Bulk $\delta^{13}C$ values of biomass were higher than in the corresponding fecal pellets (Table 2; Fig. 2B). Molar C : N ratios of zooplankton biomass ranged from 2.0 to 8.2, varying across species (Table 2; Fig. 2C). Fecal pellets mostly had a higher C : N ratio than the corresponding zooplankton biomass, (Table 2; Fig. 2C). The single low bulk $\delta^{13}C$ value and high C : N ratio in zooplankton relative to fecal pellets was found in the NE Pacific *S. aspera* samples.

Amino acid compound-specific $\delta^{15}N$ values

$\delta^{15}N$ values of Phe in zooplankton biomass ranged from −1.1‰ to 2.6‰, varying across study sites and zooplankton species (Table 2; Fig. 2D). $\delta^{15}N$ values of Phe in fecal pellets were generally similar to or lower than those of the biomass (Δzoop-FP −0.1‰ to 2.7‰; Table 2) with the exception of the two salp samples, in which fecal pellets had significantly higher Phe $\delta^{15}N$ values than biomass. The full set of compound-specific amino acid $\delta^{15}N$ values can be found in Table S2. Overall, the zooplankton biomass CSIA-AA data, when normalized to Phe $\delta^{15}N$ values, were similar to other reported values for zooplankton biomass (Hannides et al. 2020).

The CSIA-AA derived trophic position of zooplankton biomass measured here ranged from approximately 2 to 3 (Fig. 2E; Table 2), matching expectations for a mixture of primary and secondary consumers (Hannides et al. 2013, 2020). Fecal pellets had a trophic position approximately 0–1 lower than corresponding zooplankton biomass ($\Delta TP_{zoop\text{-}FP}$ of −0.2–1.1 ± 0.2). The salp and *E. superba* samples had trophic position near 2, or a primary consumer trophic position (1.7, 2.0, and 2.2 ± 0.2, respectively). The Sargasso mixed communities had trophic positions 2.3–2.6 ± 0.2; the 1–2.5 mm size class had a higher trophic position than the other two size classes. *V. propinqua*, an amphipod from the NE Pacific, had a biomass trophic position of 2.5 ± 0.2 while their fecal pellets had a trophic position of 2.0 ± 0.2 (Table 2; Fig. 2E). These *V. propinqua* were collected with the *S. aspera* in the NE Pacific and were observed in situ attached to salps (as imaged by the Underwater Video Profiler, UVP5).

Statistical results

Our ANOVA analysis helped to identify which of the CSIA data were most important in distinguishing fecal pellets from other types of organic matter. The ΣV calculation was not significantly different between end-member groups ($p > 0.05$; Table S3). All Phe-normalized amino acids were significantly different ($p < 0.05$; Supplementary Table S3) amongst the four organic matter end-member groupings. Pairwise comparison of end-member data showed that individual amino acids had a different level of skill in distinguishing particular end-member pairs (*p*-values, ANOVA, and Tukey HSD; Table S3). Notably, normalized Ala and Leu $\delta^{15}N$ values were significantly different across all end-member pairs except microbially degraded organic matter and fecal pellets (Fig. 3). The Phe-normalized $\delta^{15}N$ values of Thr and Glx were the only variables that distinguished microbially degraded organic matter and fecal pellets (Fig. 3).

Discussion

The goal of this work was to determine if fecal pellets could be reliably distinguished as a marine organic matter end-member using amino acid stable isotopic compositions. This method would allow for quantitative estimates of fecal pellet contribution to carbon export in the ocean and could improve models of the biological pump. Below, we demonstrate how the CSIA-AA approach is an improvement on previous bulk stable nitrogen isotope approaches; bulk isotope ratios are ultimately a combination of trophic and source nitrogen isotope effects, while CSIA-AA can eliminate variability due to the $\delta^{15}N$ value of nitrogen source. We also present, to our knowledge, the first trophic position calculation of fecal pellets and discuss how this value, in comparison to zooplankton trophic position, could be used to estimate the absorption efficiency of zooplankton and, thus, the relative impact of their fecal pellets on the biological pump. While quantitative mixing models have been extensively developed for carbon isotope ratios of amino acids (Larsen et al. 2015), the same development has only recently been proposed for nitrogen isotope ratios (Wall et al., 2021). We compare the ability of nine amino acids to statistically distinguish fecal pellets, zooplankton biomass, phytoplankton, and microbially degraded organic matter from one another and suggest hypotheses for why Thr and Ala are the most useful of these amino acids.

Improved interpretation of fecal pellet bulk isotope ratios

Altabet and Small (1990) interpreted the difference between zooplankton and fecal pellet $\delta^{15}N$ values ($\Delta\delta^{15}N_{zoop\text{-}FP}$) as a consequence of the offset in trophic position from zooplankton diet to biomass. They calculated an "apparent food" $\delta^{15}N$ value for each sample by subtracting 3.4‰ from the zooplankton bulk $\delta^{15}N$ value, based on consistent dietary

Table 2. Results of bulk isotope, carbon-to-nitrogen ratio, and CSIA-AA analyses for paired zooplankton (zoop) and fecal pellet (FP) samples, including the difference between zooplankton and fecal pellets for each value ($\Delta_{zoop\text{-}FP}$).

	Bulk stable isotope ratio (‰, ± 0.2)				Bulk carbon to nitrogen ratio (C : N)		Trophic position (± 0.2)		Phenylalanine δ^{15}N value (‰)		$\Delta_{zoop\text{-}FP}$				
Species	δ^{15}N Zoop	δ^{15}N FP	δ^{13}C Zoop	δ^{13}C FP	Zoop	FP	Zoop	FP	Zoop	FP	$\Delta\delta^{15}$N	$\Delta\delta^{13}$C	ΔC : N	ΔTP	$\Delta\delta^{15}$N Phe
Southern Ocean *E. superba*	3.9	1.8	−27.2	−28.1	2.0	4.8	2.2	1.4	2.6±1.3	1.6±1.0	2.1	0.9	−2.8	0.8	1.0
NE Pacific *V. propinqua*	1.6	2.1	−25.2	−27.3	2.9	4.5	2.5	2.1	1.3±0.6	0.3±1.0	−0.5	2.1	−1.6	0.4	1.0
NE Pacific *S. aspera*	0.3	−1.5	−23.1	−22.5	5.7	4.4	2.0	0.9	0.2±0.2	2.7±0.7	1.8	−0.6	1.3	1.1	−2.5
Sargasso Sea *Salpa* sp.	0.7	4.8	−22.4	−25.0	8.2	11.1	1.7	1.4	−1.1±0.3	3.3±1.0	−4.1	2.6	−2.9	0.3	−4.4
Sargasso Sea Mixed 0.25–1 mm	5.1	4.9	−22.4	−22.9	5.7	6.7	2.2	2.3	1.7±0.5	0.4±1.0	0.2	0.5	−0.9	0.1	1.3
Sargasso Sea Mixed 1–2.5 mm	5.5	5.7	−22.1	−23.1	4.4	7.0	2.4	2.6	1.4±0.1	1.5±1.0	−0.2	1.0	−2.6	−0.2	−0.1
Sargasso Sea Mixed > 1 mm	6.3	3.4	−21.2	−24.7	4.3	6.9	2.6	2.3	2.6±1.0	−0.2±0.1	2.9	3.5	−2.6	0.3	2.7

fractionations established by Deniro and Epstein (1981), McCutchan et al. (2003), and others. They argued that the bulk δ^{15}N value of fecal pellets should have a consistent offset from this "apparent food" value if the trophic isotope effect in the gut is what drove the δ^{15}N values of fecal pellets. The authors found a relatively consistent difference between "apparent food" and fecal pellet bulk δ^{15}N values of 1.9‰ to 2.4‰, equivalent to bulk $\Delta\delta^{15}N_{zoop\text{-}FP}$ values of 1.0‰ to 1.5‰. This interpretation, however, assumes that there is a consistent isotopic fractionation in the gut.

Our bulk $\Delta\delta^{15}N_{zoop\text{-}FP}$ results cannot be entirely explained by such trophic fractionation; our CSIA-AA results instead suggest dynamic dietary sources as a driver of bulk δ^{15}N values for some zooplankton and fecal pellets we characterized. First, instead of a positive value, the Sargasso Sea salps had a large negative bulk $\Delta\delta^{15}N_{zoop\text{-}FP}$. This $\Delta\delta^{15}N_{zoop\text{-}FP}$ value of −4.1‰ aligns with a Phe $\Delta\delta^{15}N_{zoop\text{-}FP}$ value of −4.4‰ (Fig. 4). The same pattern of aligned Phe and bulk $\Delta\delta^{15}N_{zoop\text{-}FP}$ values is observed in the Sargasso mixed community >1 mm. Mompeán et al. (2016) also found a strong linear relationship ($r^2 = 0.733$) between bulk δ^{15}N values and Phe δ^{15}N values of zooplankton along a transect of the North Atlantic, but a weak relationship ($r^2 = 0.475$) between normalized bulk δ^{15}N values and trophic position.

Feces in animals can include a combination of undigested dietary material, enteric bacteria, some metabolites (Harvey et al. 1989; Prahl et al. 1984), and animal biomass waste (cells of the animal). If the undigested material had a bulk value of $\delta^{15}N_{zooplankton}$ –3.4‰, and the animal biomass waste cells had the same value as $\delta^{15}N_{zooplankton}$, the possible range of bulk $\Delta\delta^{15}N_{zoop\text{-}FP}$ due to trophic fractionation is 0–3.4‰. In other words, $\Delta\delta^{15}N_{zoop\text{-}FP}$ due to $\Delta TP_{zoop\text{-}FP} = 3.4 \times \Delta TP_{zoop\text{-}FP}$. In most samples, the bulk $\Delta\delta^{15}N_{zoop\text{-}FP}$ value falls between the Phe $\Delta\delta^{15}N_{zoop\text{-}FP}$ value and $3.4 \times \Delta TP_{zoop\text{-}FP}$ (Fig. 4). The Sargasso mixed community 1–2.5 mm has overlapping Δ values for Phe $\Delta\delta^{15}N_{zoop\text{-}FP}$, bulk $\Delta\delta^{15}N_{zoop\text{-}FP}$, and $3.4 \times \Delta TP_{zoop\text{-}FP}$.

In incubation experiments, Tamelander et al. (2006) found that copepods undergoing a change in diet retained their initial biomass bulk δ^{15}N value as long as 30 d. If the turnover time for bulk δ^{15}N values in biomass exceeds the time of a change in diet, the δ^{15}N values of diet and biomass may be decoupled. CSIA-AA helps to test this hypothesis: in the Sargasso *Salpa* sp., a large negative bulk $\Delta\delta^{15}N_{zoop\text{-}FP}$ value corresponds with a large negative Phe $\Delta\delta^{15}N_{zoop\text{-}FP}$ value (Table 2; Figs. 2D, 3). Because Phe maintains the δ^{15}N value of the nitrogen source at the base of the food web (McClelland and Montoya 2002; Chikaraishi et al. 2007), a Phe $\Delta\delta^{15}N_{zoop\text{-}FP}$ value of 0.4‰ ± 0.5‰ (i.e., the small isotopic fractionation expected at each trophic transfer) would be expected at steady state. Therefore, we suggest that the source of nitrogen to the salp biomass was different than the source of nitrogen to fecal pellets due to a change in diet on a timescale shorter than average salp tissue turnover. This could be caused by a short timescale change in salp diet due to vertical migration or a

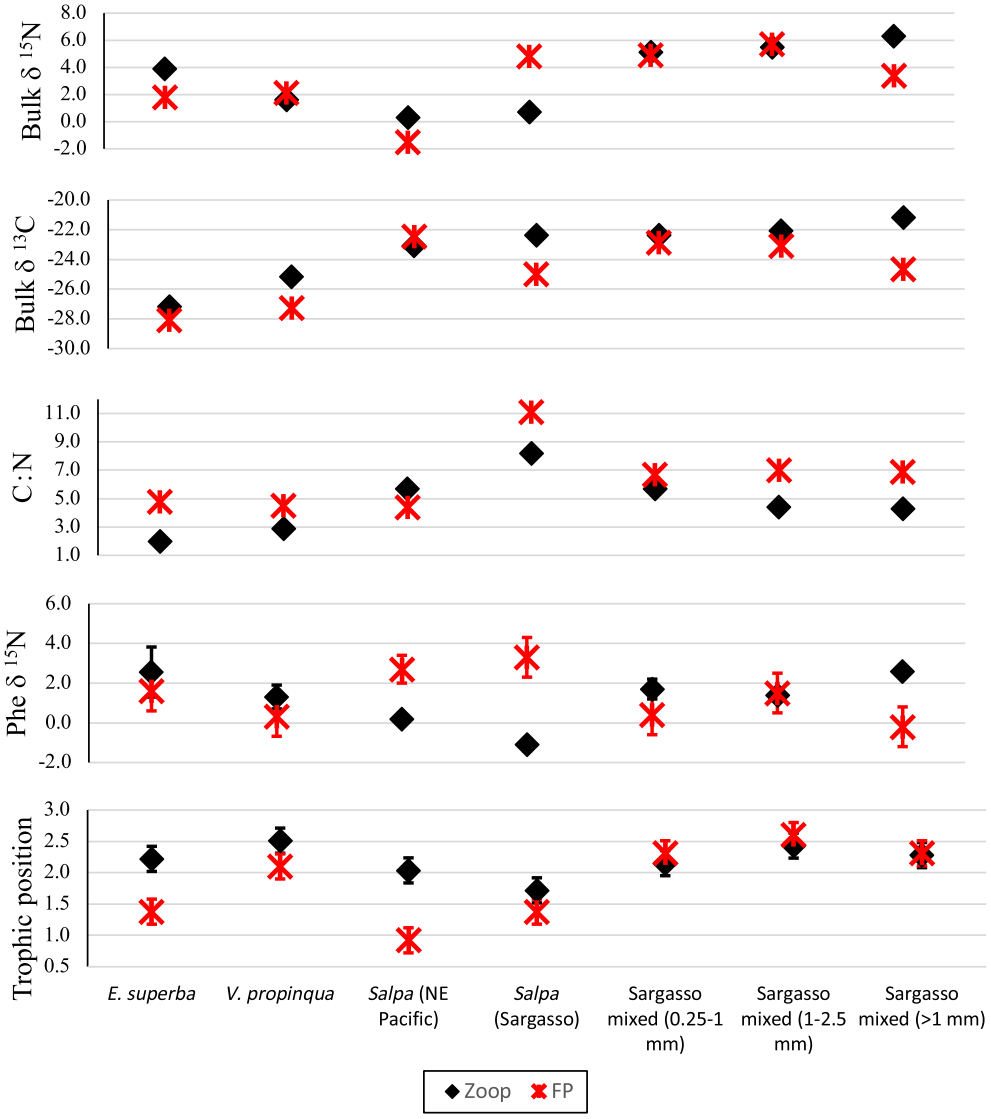

Fig. 2. Bulk $\delta^{15}N$ values (a), phenylalanine (Phe) $\delta^{15}N$ values ($\delta^{15}N_{Phe}$; b), carbon-to-nitrogen molar ratio (C:N; c), bulk $\delta^{13}C$ values (d), and CSIA-determined trophic position (TP; e) for zooplankton (black diamonds) and fecal pellet (red stars) samples. Error bars indicate $\pm 1\sigma$ analytical uncertainty and are not visible if the marker size is larger than the uncertainty.

phytoplankton bloom, which could cause the fecal pellets to have the relatively higher $\delta^{15}N$ values of the most recent diet, while the salp tissue has the lower $\delta^{15}N$ value of the average integrated diet. When considering temporal changes in diet, potential dietary sources with relatively high $\delta^{15}N$ values include mesopelagic particulate organic matter (Altabet et al. 1991) or more nitrate-based production (Sigman et al. 2009). Potential dietary sources with relatively low $\delta^{15}N$ values, by comparison, include epipelagic particulate organic matter (Altabet et al. 1991) or more ammonium or N_2-based production (Sigman et al. 2009). Better characterization of local planktonic and particulate food resources would aid in interpretation of potential heterogeneous dietary resources.

In the NE Pacific *S. aspera*, and Sargasso mixed community 0.25–1 mm samples, bulk $\Delta\delta^{15}N_{zoop\text{-}FP}$ appears to be influenced both by source differences and trophic position differences between zooplankton and fecal pellets (Fig. 3). Therefore, trophic position and the $\Delta\delta^{15}N$ value of the source nitrogen both influence the bulk $\Delta\delta^{15}N_{zoop\text{-}FP}$ (see below).

The bulk $\Delta\delta^{15}N_{zoop\text{-}FP}$ value of the > 1 mm Sargasso mixed community also was larger in magnitude than what would be expected from the trophic offset found by Altabet and Small (1990). In this case, the bulk $\Delta\delta^{15}N_{zoop\text{-}FP}$ was also similar to that of the Phe $\Delta\delta^{15}N_{zoop\text{-}FP}$ value (2.9‰ ± 0.2‰ and 2.7‰ ± 1.0‰, respectively), although opposite in sign to the salps (Table 2; Fig. 3). This bulk $\delta^{15}N$ offset between fecal

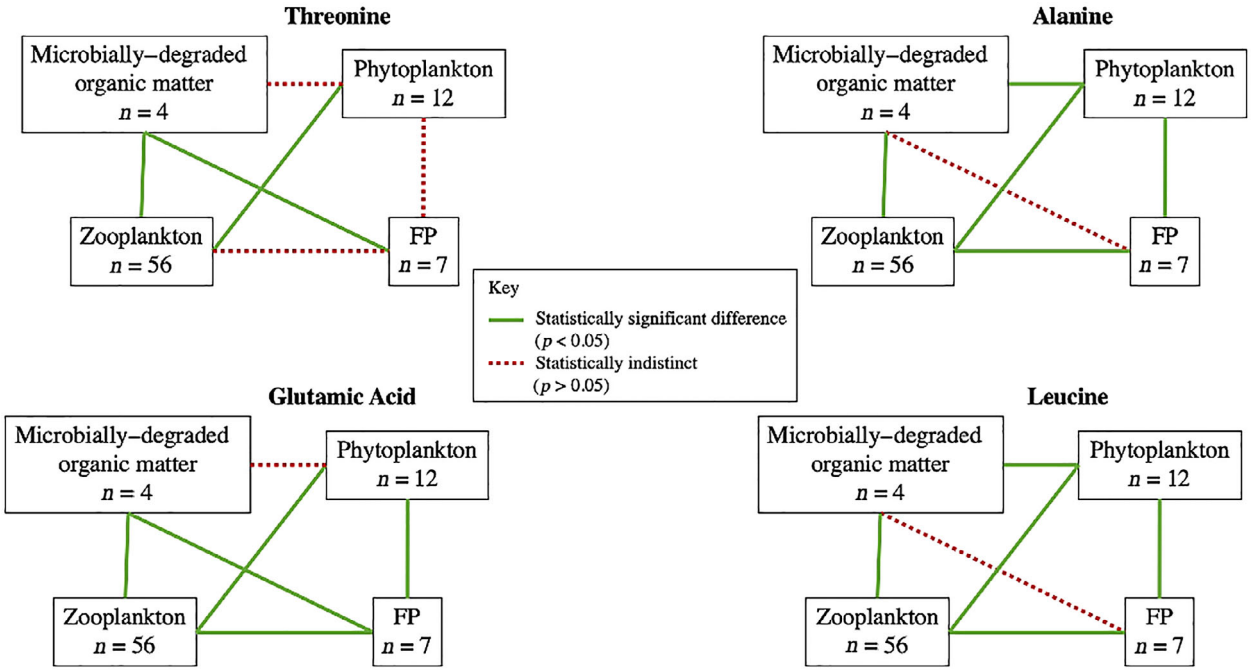

Fig. 3. Results of Tukey HSD for pairwise comparison of end-member groups for the amino acids threonine, alanine, glutamic acid, and leucine. Significant differences between end-members are shown in green, solid connecting lines and statistically indistinct end-members are connected by a dotted, red line.

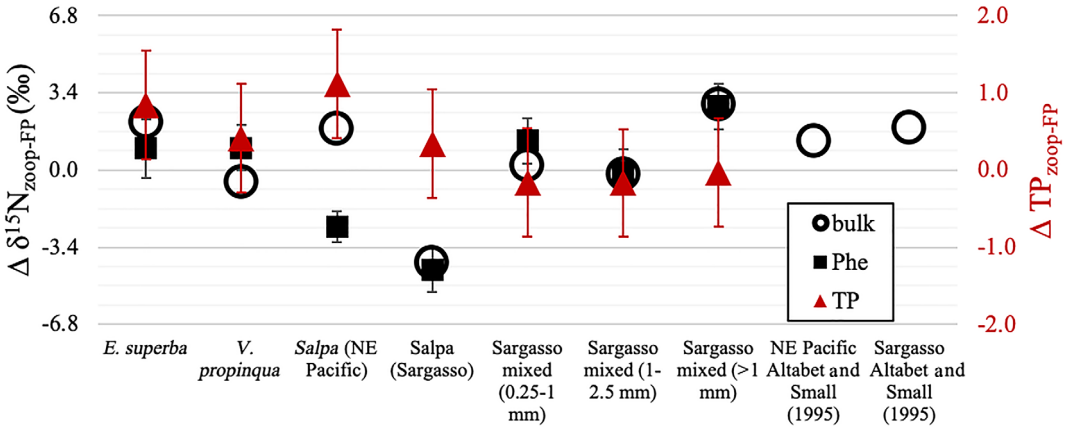

Fig. 4. The difference between zooplankton and fecal pellets (Δzoop-FP) in: bulk $\delta^{15}N$ value (open black circle), Phe $\delta^{15}N$ value (black square), trophic position (TP) (red triangle, secondary y-axis). A bulk $\delta^{15}N$ shift of 3.4‰ is commonly interpreted in animal food webs as reflecting one trophic level; the secondary axis for CSIA-AA derived trophic position has been scaled to a $\delta^{15}N$ value of 3.4 here so that it is equivalent to the expected trophic shift in bulk $\delta^{15}N$ values. Error bars indicate $\pm$ 1σ analytical uncertainty and are not visible if the marker size is larger than the uncertainty. Bulk isotope data from Altabet and Small (1990) are included for comparison; symbol size encapsulates the range observed for multiple samples from each of two regions in that study.

pellets and biomass could also represent a temporal change in diet, but in this case the recent diet would have lower $\delta^{15}N$ values than the integrated animal diet.

These results suggest that (1) trophic dynamics between an animal and its fecal pellets cannot be determined using bulk $\delta^{15}N$ values alone and (2) instead nitrogen source in the recent diet and/or alteration by gut microbiota is the primary driver of bulk $\delta^{15}N$ values in fecal pellets.

Higher bulk $\delta^{13}C$ values in zooplankton relative to fecal pellets (Table 2; Fig. 2B) also could indicate a trophic enrichment, although most zooplankton samples were enriched in ^{13}C relative to fecal pellets well above the 0.5‰ expected from a trophic shift (McCutchan et al. 2003). Changes in $\delta^{13}C$ values can also indicate compositional changes: either a change in diet over time or a difference in the chemical composition from diet to biomass. Tamelander et al. (2006)

measured stable isotopic composition of copepods, their diet, and their fecal pellets in a feeding study and reported lower $\delta^{13}C$ values in fecal pellets compared to diet, indicating preferential removal of compounds with higher $\delta^{13}C$ values during digestion. We also found that nitrogen was preferentially removed from the diet, into biomass; fecal pellets mostly had a higher C : N ratio than the corresponding zooplankton biomass, (Table 2; Fig. 2C). The single low bulk $\delta^{13}C$ value and high C : N ratio in zooplankton relative to fecal pellets was found in the NE Pacific *S. aspera* samples and may be a result of less complete digestion in this sample than in others we measured. The relative trophic position of biomass and fecal pellets in this sample also suggests inefficient digestion of the NE Pacific salps (below).

Trophic position and zooplankton communities

Our zooplankton trophic position values generally fell in the expected range of mesozooplankton trophic position of 2–3. In the Sargasso mixed communities, a trophic position of 2–3 could result from a mixed community engaging in grazing, detritivory, and some carnivory of smaller zooplankton (Schnetzer and Steinberg 2002). Interestingly, all three size classes of zooplankton had similar trophic position, indicating similar overall dietary strategies. Active carnivory was observed in the experimental containers for the 1–2.5 mm size class, which is perhaps the cause of the relatively high trophic position we observed in the corresponding fecal pellets (2.6 ± 0.2; Table 2; Fig. 2E): the fecal pellets contain animal biomass.

Although obtained from disparate locations, both samples of *Salpa* sp. had a biomass trophic position near 2 (2.0 and 1.7 ± 0.2, NE Pacific and Sargasso, respectively; Table 2; Fig. 2E), as would be expected from zooplankton feeding primarily on phytoplankton and phytodetritus (Madin 1982). In contrast to the mixed community samples, the trophic position of *Salpa* sp. fecal pellets were significantly lower than their biomass (trophic position of 0.9 and 1.4 ± 0.2, NE Pacific and Sargasso, respectively; Table 2; Fig. 2E). *E. superba* collected during austral summer from the Southern Ocean, like the NE Pacific salps, had a biomass trophic position of approximately 2 (2.2 ± 0.2), indicating these zooplankton were primarily feeding on phytoplankton, and a lower trophic position of fecal pellets (1.4 ± 0.2; Table 2; Fig. 2E).

V. propinqua are known to be specific and obligate parasites of salps; at different stages during their life cycle *V. propinqua* feed on both the salp tissue and the particulate organic matter collected in the mucous net of the salp (Madin and Harbison 1977). With the expectation that the *V. propinqua* had access to feed on both the salp tissue (trophic position 2.0 ± 0.2) and the salps' dietary materials (inferred trophic position of 1.0), their trophic position of 2.5 ± 0.2 suggests that they indeed feed on both. Because our *V. propinqua* analysis included a homogenized collection of individuals, it is possible that this represents an integrated trophic position of both juveniles, which feed on salp tissue, and adults, which feed on the salp's diet of particulate organic matter (Madin and Harbison 1977).

ΔTP as a measure of digestion efficiency in zooplankton

As stated above, feces in animals can include a combination of undigested dietary material, enteric bacteria, metabolites, and animal biomass waste (cells of the animal). When considering how these components would influence the trophic position of zooplankton fecal pellets, we hypothesize that undigested dietary material would retain the diet's trophic position (approximately $TP_{zooplankton} - 1$). This would include any material that has neither been digested nor absorbed by either the zooplankter or their enteric bacteria. In contrast, material that is absorbed into zooplankton biomass would undergo isotopic fractionation during catabolism, resulting in a higher trophic position (Chikaraishi et al. 2009). Therefore, we hypothesize that zooplankton biomass waste that contributes to fecal pellets would have the same trophic position as the zooplankton body. We hypothesize that the enteric bacteria feeding on gut contents could also have the same trophic position as the zooplankton body or higher; heterotrophic microbes fractionate the nitrogen isotopes of amino acids similar to animal consumers when catabolizing amino acids instead of synthesizing them (Yamaguchi et al. 2017).

We therefore posit that the difference in the trophic position of fecal pellets and corresponding zooplankton biomass, $\Delta TP_{zoop\text{-}FP}$, indicates the relative proportion of undigested dietary material vs. enteric bacteria and animal cells in fecal pellets. $\Delta TP_{zoop\text{-}FP}$ thus could indicate the relative composition of fecal pellets: A $\Delta TP_{zoop\text{-}FP}$ near 1 would suggest that the proteinaceous material in the fecal pellets is primarily made of undigested dietary material (Fig. 5), meaning that the majority of fecal pellet contents would have the signature of undigested dietary material (approximately $TP_{zooplankton} - 1$). A $\Delta TP_{zoop\text{-}FP}$ of 0 would suggest that the proteinaceous material in the fecal pellets is primarily derived from organic matter metabolized by enteric bacteria and/or zooplankton, as these fecal pellet components are expected to have the same trophic position as the zooplankton (Fig. 4). Interpreting $\Delta TP_{zoop\text{-}FP}$, therefore, is similar to interpreting absorption efficiency. While absorption efficiency in zooplankton is typically a direct measure of the proportion of dietary carbon zooplankton absorbed across their gut walls (Steinberg and Landry 2017), $\Delta TP_{zoop\text{-}FP}$ approximates the proportion of dietary material that passed through the gut undigested. However, the $\Delta TP_{zoop\text{-}FP}$ calculation can only be interpreted this way if the zooplankton and fecal pellets are in steady state, that is, if they are derived from the same dietary source. In this study we interpret pairs as "in steady state" if their Phe $\Delta\delta^{15}N_{zoop\text{-}FP}$ values are within the analytical uncertainty range of a value of 0.4‰. Samples meeting this condition included *E. superba*, *V. propinqua*,

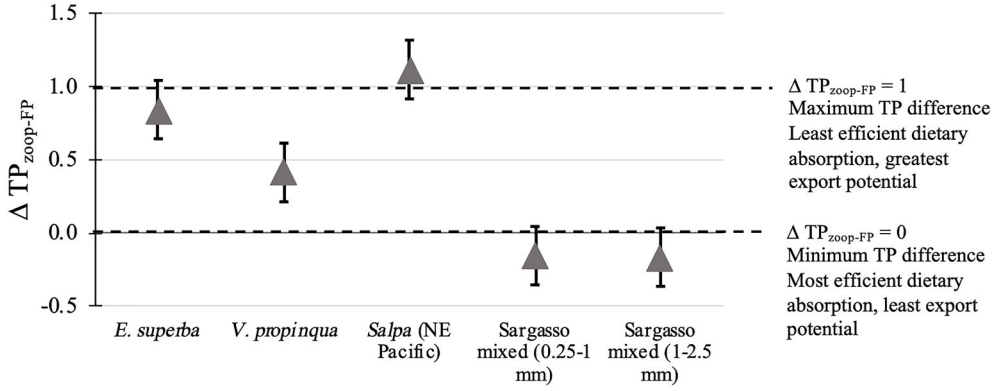

Fig. 5. Difference in CSIA-determined trophic position ($\Delta TP_{zoop\text{-}FP}$) for all presumed steady- state samples with dashed lines highlighting the theoretical maximum ($\Delta TP_{zoop\text{-}FP} = 1$) and minimum ($\Delta TP_{zoop\text{-}FP} = 0$). Text indicates our proposed interpretation of this metric with regard to zooplankton absorption efficiency and potential carbon export. Greater or lesser export potential refers to the mass of carbon remaining in the fecal pellets after digestion and not to the actual flux.

Sargasso mixed 0.25–1 mm and Sargasso mixed 1–2.5 mm. We also include the *S. aspera* samples from the NE Pacific, which have a theoretical maximum $\Delta TP_{zoop\text{-}FP}$ and therefore would be interpreted similarly regardless of steady state.

If $\Delta TP_{zoop\text{-}FP}$ can be used as an indicator of the efficiency of zooplankton digestion, we suggest it also reflects the potential efficiency of fecal pellet packaging as a vector of the biological pump. Export models often involve a food web component (Michaels and Silver 1988; Siegel et al. 2014), which estimates fecal pellet contribution to carbon export based on parameters that capture the fraction of dietary carbon that is egested after zooplankton digestion. Absorption efficiency can also be used to determine the potential organic carbon content of fecal pellets after they are egested by zooplankton (Steinberg and Landry 2017). Combined, the grazing rate of zooplankton and their absorption efficiency can be used to determine carbon exported by fecal pellets from primary production. However, the efficiency of zooplankton digestion—and therefore the proportion of undigested material in fecal pellets—is variable, even in a single species and region (Atkinson et al. 2012). If higher values of $\Delta TP_{zoop\text{-}FP}$ indicate low efficiency of animal digestion, then they also indicate greater fecal packaging of undigested, lower-trophic position material (Fig. 5). Because each trophic step in a food chain (measured as trophic position) involves the catabolic loss of dietary carbon as CO_2, fecal packaging of lower-trophic position material (higher values of $\Delta TP_{zoop\text{-}FP}$) should also represent greater overall carbon export potential. This packaging of undigested material may be exported to depth and serve as a high-quality food source for midwater organisms.

Using the reasoning above, near-zero values of $\Delta TP_{zoop\text{-}FP}$ for the two steady state Sargasso mixed community samples (Fig. 5) suggest that these zooplankton communities as a whole efficiently digested their diet and expelled very little undigested dietary material in their fecal pellets. This may reflect a high net dietary efficiency of a mixed community engaging in herbivory, carnivory, and detritivory.

The large $\Delta TP_{zoop\text{-}FP}$ of the NE Pacific salps suggests that they have a large proportion of undigested dietary material in their fecal pellets ($\Delta TP_{zoop\text{-}FP} = 1.1 \pm 0.2$). The fecal pellets of NE Pacific *Salpa* sp. had a relatively low C : N ratio of 4.4, indicating fresher organic matter (Table 2; Fig. 2). In addition, salp biomass also had a higher C : N ratio and a lower bulk $\delta^{13}C$ value relative to fecal pellets (Fig. 2B), unlike any other zooplankton-fecal pellet pair, which may both point to a lack of digestive processing of the recent diet for these salps. These salps' lower bulk $\delta^{13}C$ value of biomass relative to fecal pellets could also be due to a shift in phytoplankton diet as discussed above; different phytoplankton species have different $\delta^{13}C$ values (Popp et al. 1998).

Inefficient digestion and efficient export by salps in the NE Pacific during the same sampling period (EXPORTS) is also indicated by our observation of undigested phytoplankton cells in salp fecal pellets. During the EXPORTS cruise, salp fecal pellets contributed a large proportion of particle mass collected in sediment traps whenever *S. aspera* were present in the water column (Durkin et al., 2021). It is notable that the net impact on export potential of fecal pellet production by salps is of particular importance due to their feeding mode, which captures small, otherwise nonsinking or slowly sinking particles and repackages them into large, dense pellets that sink quickly (Madin 1982). This packaging would generate a method by which the organic matter in small particles could be rapidly transported to the mesopelagic. Incubations of salp fecal pellets conducted by Caron et al. (1989) and during the EXPORTS cruise (Steinberg et al. in prep.) suggest that salp fecal pellets are unlikely to be significantly altered by heterotrophic microbes as they sink, and therefore they could also be a vector of high-quality organic matter to the mesopelagic zone.

With a $\Delta TP_{zoop\text{-}FP}$ near 1 (0.8 ± 0.2), *E. superba* sampled here may have been eliminating mostly undigested food (Fig. 5). This has been observed previously in *E. superba* fecal pellets; Belcher et al. (2017) noted that *E. superba* fecal pellets in locations with high transfer efficiency contained fresh phytodetritus. Atkinson et al. (2012) also noted that during "high egestion" phases (i.e., high fecal pellet production phases), *E. superba* tend to have a diet higher in diatoms and lower in microzooplankton. Fast-sinking *E. superba* fecal pellets dominate summer carbon flux in the Southern Ocean (Cavan et al. 2015; Belcher et al. 2017) and in the region we sampled comprise 82% of the sinking particulate organic carbon collected in sediment traps during summer (Gleiber et al. 2012). Therefore, these fecal pellets are a major driver of the biological pump, packaging phytodetritus and exporting it quickly to the mesopelagic. A $\Delta TP_{zoop\text{-}FP}$ near 1 confirms this fecal pellet composition. However, Atkinson et al. (2012) also found that *E. superba* fecal pellets with higher proportions of undigested material sank more slowly than fecal pellets with less undigested material, thereby exposing them to longer timespans of biological degradation. The relative density of fecal pellets with different undigested proportions thus can also ultimately impact fecal pellet export efficiency.

With a $\Delta TP_{zoop\text{-}FP}$ of 0.4 (Fig. 5), the *V. propinqua* appear to have had moderately efficient digestion. This could be due to their insulation from environmental conditions as parasites living on NE Pacific salps; the availability of food to parasitic *V. propinqua* thus places them between superfluous (such as *E. superba*) and near-starvation (such as the Sargasso mixed community) food levels.

Zooplankton fecal pellets as a component of particulate material

The four end-members we compiled from previously published amino acid $\delta^{15}N$ data and this study—fecal pellets, zooplankton biomass, phytoplankton biomass, and microbially degraded organic matter—all potentially contribute to particulate organic matter in the ocean. Our goal was to determine which, if any, amino acids reliably distinguished these end-members from one another. We found that Thr and Ala were the most promising compounds owing both to their ability to resolve end-members statistically and the existence of theoretical bases for these metabolic distinctions.

While both Thr and Glx were able to statistically distinguish fecal pellets from microbially degraded organic matter, Thr is likely the better of the two at separating these end-members due to its distinct metabolic fractionation in animal metabolisms. Animal metabolic processes impart a low $\delta^{15}N$ value on Thr (Gaebler et al. 1966; McMahon and McCarthy 2016), while the same signature has not been demonstrated for microbial metabolic processes (Fuller and Petzke 2017). Mompeán et al. (2016) also found that Phr-normalized Thr $\delta^{15}N$ values of zooplankton demonstrated a negative relationship with all proxies of trophic transfer; linear regressions between Phr-normalized Thr $\delta^{15}N$ varied by region. When Phe-normalized Thr $\delta^{15}N$ values of high molecular weight dissolved organic matter, phytoplankton, zooplankton, and fecal pellets were compared, both fecal pellets and zooplankton had low Phe-normalized $\delta^{15}N$ Thr values relative to high molecular weight dissolved organic matter and phytoplankton (Fig. 6). That is, end-members involved in animal metabolism (zooplankton and fecal pellets) were

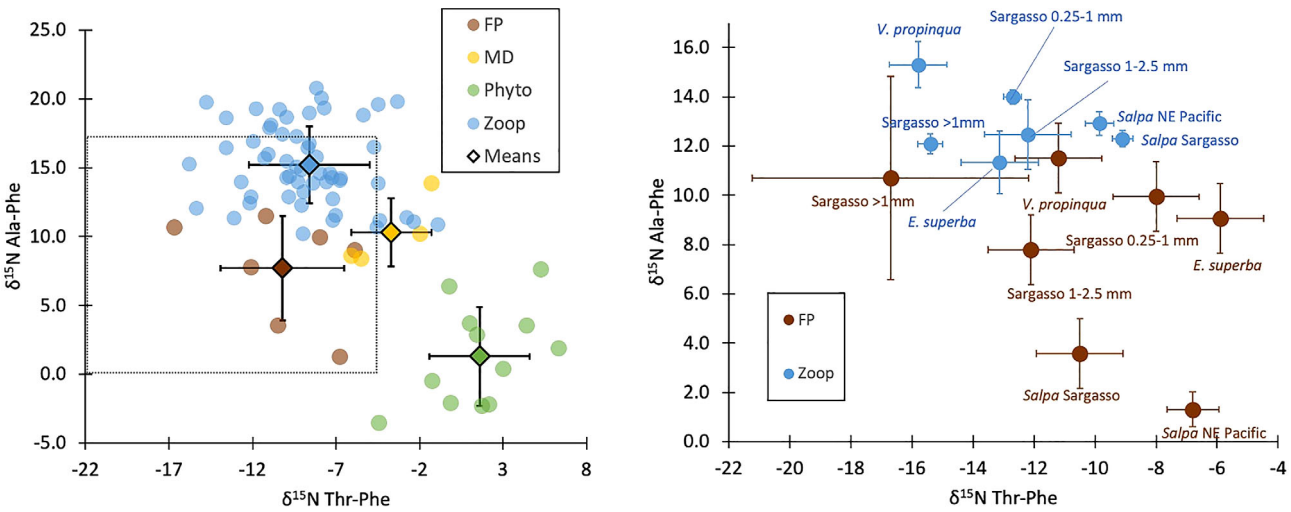

Fig. 6. (**A**) End-member (fecal pellets, FP; microbially degraded, MD; phytoplankton; and zooplankton) data of phenylalanine (Phe)-normalized threonine (Thr) and alanine (Ala) $\delta^{15}N$ values (semi-transparent circles) with end-member means and standard deviations (diamonds with error bars). Fecal pellets and some zooplankton data are from this study. Other data are from published studies, detailed in Table S3. (**B**) Inset of plot A, highlighting only labeled zooplankton and fecal pellet samples from this study. Error bars represent the propagated error of the Ala-Phe and Thr-Phe calculations.

distinguished from those involved in microbial metabolism (phytoplankton and microbially degraded). Therefore, even relatively undigested fecal material (samples with high $\Delta TP_{zoop\text{-}FP}$) likely undergoes some alteration in the gut. In contrast, the difference in Phe-normalized $\delta^{15}N$ Glx values between fecal pellets and microbially degraded organic matter end-members is likely due to a difference in trophic position between the means of these two groups, and therefore would not be as robust in a case where the trophic positions were similar.

Similarly, although both Ala and Leu were successful at statistically differentiating some end-member materials, we suggest that Ala has a stronger theoretical basis for end-member separation. The $\delta^{15}N$ values of Ala, a trophic amino acid, increase as organic matter moves up the food web, across all types of consumers (Décima et al. 2017). However, the nitrogen isotopic fractionation of Ala appears to be more sensitive to the microbial food web than Glx (demonstrated in phagotrophic protists; Gutiérrez-Rodríguez et al. 2014; Décima et al. 2017), which could be especially important when microzooplankton are dietary items of mesozooplankton. This concept also is supported by the better ability of Ala $\delta^{15}N$ values than those of Glx in distinguishing between phytoplankton and microbially degraded end-members (Table S3). When Phe-normalized Ala $\delta^{15}N$ values of the four end-members were compared, zooplankton had the highest $\delta^{15}N$ values, phytoplankton had the lowest $\delta^{15}N$ values, and microbially degraded organic matter and fecal pellets fell between the two (Fig. 6). Here, materials most clearly influenced by heterotrophy (microbially degraded organic matter and primary and secondary consumer biomass) had higher Phe-normalized Ala $\delta^{15}N$ values, while the low Phe-normalized Ala $\delta^{15}N$ values of phytoplankton are consistent with primary producers. Fecal pellets likely fall between these groups because they contain heterotrophic signatures from zooplankton biomass and gut microbiota as well as primary signatures from undigested phytodetritus.

Combined, Phe-normalized Thr and Ala $\delta^{15}N$ values create a two-dimensional separation of all four end-members (Fig. 6). This separation suggests that this method of sorting metabolisms could be useful in determining the relative contribution of these end-members to bulk collections of detrital organic matter like particulate organic matter or sedimentary organic matter. Because these parameters are internally normalized to Phe $\delta^{15}N$ values, similar to trophic position, samples from different regions or sources can be compared directly.

We draw a comparison to amino acid carbon isotope fingerprinting, which has been used to quantify the contribution of various primary producers to organisms' diets or organic composites (Larsen et al. 2013; Vokhshoori et al. 2014; McMahon et al. 2015; Jarman et al. 2017). Bayesian isotope mixing models are employed to estimate the contribution of various possible primary producer end-members to a mixture. We suggest that nitrogen CSIA-AA can be used in a similar Bayesian isotope mixing model, such as SIAR or FRUITS, with Phe-normalized Thr and Ala $\delta^{15}N$ values to quantify the contribution of organic matter end-members to particulate organic matter based on metabolic signatures, and therefore include the contribution of fecal pellets to organic matter pools in the ocean. More data representing end-members, microbially degraded organic matter in particular, is necessary before the implementation of a Bayesian mixing model. The fecal pellet end-members in this study represent "fresh" fecal pellets; fecal pellets that have been exposed to degradation in the water column should also be considered in future work. We suggest that further refinement of this end-member separation may be achieved in the future with the addition of carbon CSIA-AA data; this may improve the distinction of signatures deriving from gut vs. water column bacteria and therefore improve the distinction between fecal pellets and microbially degraded particulate organic matter.

Conclusions

We explored stable isotopic and trophic commonalities between mixed community and species-specific samples of zooplankton and their fecal pellets from three distinct oceanographic regions. We reach four major conclusions:

- Nitrogen source in the recent diet (including different phytoplankton communities or feeding at different depths) and/or alteration by gut microbiota is the primary driver of bulk $\delta^{15}N$ values in fecal pellets.
- The relative measure of $\Delta TP_{zoop\text{-}FP}$, derived from nitrogen CSIA-AA, can be used as an indicator of the efficiency of zooplankton digestion and, consequently, the potential efficiency of fecal pellets packaging as a vector of the biological pump.
- Nitrogen CSIA-AA can be used to distinguish fecal pellets from other end-members expected to contribute to marine organic matter.
- Alanine and threonine are the most useful amino acids for this end-member separation.

We suggest that future work can use Phe-normalized $\delta^{15}N$ Thr and $\delta^{15}N$ Ala values to estimate fecal pellet contribution to detrital organic matter. The variability of the $\delta^{15}N_{Thr}$ and $\delta^{15}N_{Ala}$ fecal pellet signatures across zooplankton regions and species beyond those included in this study remains unknown. The effect of environmental bacterial degradation in the water column on the CSIA-AA patterns for "aged" fecal pellets is also unknown and subject to further study. Heterotrophic microbial biomass is not captured by the organic matter end-members presented here, and may be developed with further CSIA-AA studies and the addition of carbon CSIA-AA. More work is also needed to determine the underlying causes of differences in $\Delta TP_{zoop\text{-}FP}$, which may be a factor of food availability, species-specific feeding strategies, temperature, or other environmental conditions.

References

Abramson, L., C. Lee, Z. Liu, S. G. Wakeham, and J. Szlosek. 2010. Exchange between suspended and sinking particles in the northwest Mediterranean as inferred from the organic composition of in situ pump and sediment trap samples. Limnol. Oceanogr. **55**: 725–739. doi:10.4319/lo.2009.55.2.0725

Altabet, M. A., W. G. Deuser, S. Honjo, and C. Stienen. 1991. Seasonal and depth-related changes in the source of sinking particles in the North Atlantic. Nature **354**: 136–139. doi:10.1038/354136a0

Altabet, M. A., and L. F. Small. 1990. Nitrogen isotopic ratios in fecal pellets produced by marine zooplankton. Geochim. Cosmochim. Acta **54**: 155–163. doi:10.1016/0016-7037(90)90203-W

Atkinson, A., K. Schmidt, S. Fielding, S. Kawaguchi, and P. A. Geissler. 2012. Variable food absorption by Antarctic krill: Relationships between diet, egestion rate and the composition and sinking rates of their fecal pellets. Deep. Res. Part II Top. Stud. Oceanogr. **59–60**: 147–158. doi:10.1016/j.dsr2.2011.06.008

Belcher, A., and others. 2017. The potential role of Antarctic krill faecal pellets in efficient carbon export at the marginal ice zone of the South Orkney Islands in spring. Polar Biol. **40**: 2001–2013. doi:10.1007/s00300-017-2118-z

Caron, D. A., L. P. Madin, and J. J. Cole. 1989. Composition and degradation of salp fecal pellets: Implications for vertical flux in oceanic environments. J. Mar. Res. **47**: 829–850. doi:10.1357/002224089785076118

Cavan, E. L., F. A. C. Le Moigne, A. J. Poulton, G. A. Tarling, P. Ward, C. J. Daniels, G. M. Fragoso, and R. J. Sanders. 2015. Attenuation of particulate organic carbon flux in the Scotia Sea, Southern Ocean, is controlled by zooplankton fecal pellets. Geophys. Res. Lett. **42**: 821–830. doi:10.1002/2014GL062744

Chikaraishi, Y., Y. Kashiyama, N. O. Ogawa, H. Kitazato, and N. Ohkouchi. 2007. Metabolic control of nitrogen isotope composition of amino acids in macroalgae and gastropods: Implications for aquatic food web studies. Mar. Ecol. Prog. Ser. **342**: 85–90. doi:10.3354/meps342085

Chikaraishi, Y., and others. 2009. Determination of aquatic food-web structure based on compound-specific nitrogen isotopic composition of amino acids. Limnol. Oceanogr.: Methods **7**: 740–750. doi:10.4319/lom.2009.7.740

Dagg, M. J., G. A. Jackson, and D. M. Checkley. 2014. The distribution and vertical flux of fecal pellets from large zooplankton in Monterey bay and coastal California. Deep. Res. Part I Oceanogr. Res. Pap. **94**: 72–86. doi:10.1016/j.dsr.2014.09.001

Décima, M., M. R. Landry, C. J. Bradley, and M. L. Fogel. 2017. Alanine δ^{15}N trophic fractionation in heterotrophic protists. Limnol. Oceanogr. **62**: 2308–2322. doi:10.1002/lno.10567

Deniro, M. J., and S. Epstein. 1981. Influence of diet on the distribution of nitrogen isotopes in animals. Geochim. Cosmochim. Acta **45**: 341–351. doi:10.1016/0016-7037(81)90244-1

Durkin, C.A., K.O. Buesseler, I. Cetinić, M. Estapa, R.P. Kelley, M. Omand. 2021. A visual tour of carbon export by sinking particles.

Fuller, B. T., and K. J. Petzke. 2017. The dietary protein paradox and threonine ^{15}N-depletion: Pyridoxal-5′-phosphate enzyme activity as a mechanism for the δ^{15}N trophic level effect. Rapid Commun. Mass Spectrom. **31**: 705–718. doi:10.1002/rcm.7835

Gaebler, O. H., T. G. Vitti, and R. Vukmirovich. 1966. Isotope effects in metabolism of ^{14}N and ^{15}N from unlabeled dietary proteins. Can. J. Biochem. **44**: 1249–1257. doi:https://doi.org/10.1139/o66-142

Gleiber, M. R., D. K. Steinberg, and H. W. Ducklow. 2012. Time series of vertical flux of zooplankton fecal pellets on the continental shelf of the western Antarctic Peninsula. Mar. Ecol. Prog. Ser. **471**: 23–36. doi:10.3354/meps10021

Gloeckler, K., C. A. Choy, C. C. S. Hannides, H. G. Close, E. Goetze, B. N. Popp, and J. C. Drazen. 2018. Stable isotope analysis of micronekton around Hawaii reveals suspended particles are an important nutritional source in the lower mesopelagic and upper bathypelagic zones. Limnol. Oceanogr. **63**: 1168–1180. doi:https://doi.org/10.1002/lno.10762

Gutiérrez-Rodríguez, A., M. Décima, B. N. Popp, and M. R. Landry. 2014. Isotopic invisibility of protozoan trophic steps in marine food webs. Limnol. Oceanogr. **59**: 1590–1598. doi:10.4319/lo.2014.59.5.1590

Hannides, C. C. S., B. N. Popp, C. Anela Choy, and J. C. Drazen. 2013. Midwater zooplankton and suspended particle dynamics in the North Pacific Subtropical Gyre: A stable isotope perspective. Limnol. Oceanogr. **58**: 1931–1936. doi:10.4319/lo.2013.58.6.1931

Hannides, C. C. S., and others. 2020. Seasonal dynamics of midwater zooplankton and relation to particle cycling in the North Pacific Subtropical Gyre. Prog. Oceanogr. **182**: 102266. doi:10.1016/j.pocean.2020.102266

Hannides, C. C. S., B. N. Popp, M. R. Landry, and B. S. Graham. 2009. Quantification of zooplankton trophic position in the North Pacific Subtropical Gyre using stable nitrogen isotopes. Limnol. Oceanogr. **54**: 50–61. doi:10.4319/lo.2009.54.1.0050

Harvey, H. R., S. C. M. O'Hara, G. Eglinton, and E. D. S. Corner. 1989. The comparative fate of dinosterol and cholesterol in copepod feeding: Implications for a conservative molecular biomarker in the marine water column. Org. Geochem. **14**: 635–641. doi:10.1016/0146-6380(89)90042-9

Henschke, N., J. D. Everett, A. J. Richardson, and I. M. Suthers. 2016. Rethinking the role of salps in the ocean. Trends Ecol. Evol. **31**: 720–733. doi:10.1016/j.tree.2016.06.007

Jarman, C. L., and others. 2017. Diet of the prehistoric population of Rapa Nui (Easter Island, Chile) shows environmental adaptation and resilience. Am. J. Phys. Anthropol. **164**: 343–361. doi:10.1002/ajpa.23273

Lam, P. J., and O. Marchal. 2015. Insights into particle cycling from thorium and particle data. Ann. Rev. Mar. Sci. **7**: 159–184. doi:10.1146/annurev-marine-010814-015623

Larsen, T., L. T. Bach, R. Salvatteci, Y. V. Wang, N. Andersen, M. Ventura, and M. D. McCarthy. 2015. Assessing the potential of amino acid ^{13}C patterns as a carbon source tracer in marine sediments: Effects of algal growth conditions and sedimentary diagenesis. Biogeosciences **12**: 4979–4992. doi:10.5194/bg-12-4979-2015

Larsen, T., M. Ventura, N. Andersen, D. M. O'Brien, U. Piatkowski, and M. D. McCarthy. 2013. Tracing carbon sources through aquatic and terrestrial food webs using amino acid stable isotope fingerprinting. PLoS One **8**: e73441. doi:10.1371/journal.pone.0073441

Lee, R. F., W. Hagen, and G. Kattner. 2006. Lipid storage in marine zooplankton. Mar. Ecol. Prog. Ser. **307**: 273–306. doi:10.3354/meps307273

Longhurst, A. R., and W. Glen Harrison. 1989. The biological pump: Profiles of plankton production and consumption in the upper ocean. Prog. Oceanogr. **22**: 47–123. doi:10.1016/0079-6611(89)90010-4

Madin, L. P. 1982. Production, composition and sedimentation of salp fecal pellets in oceanic waters. Mar. Biol. **67**: 39–45. doi:10.1007/BF00397092

Madin, L. P., and G. R. Harbison. 1977. The associations of Amphipoda Hyperiidea with gelatinous zooplankton. Deep. Res. **24**: 449–463. doi:10.1016/0146-6291(77)90483-0

McCarthy, M. D., J. Lehman, and R. Kudela. 2013. Compound-specific amino acid $\delta^{15}N$ patterns in marine algae: Tracer potential for cyanobacterial vs. eukaryotic organic nitrogen sources in the ocean. Geochim. Cosmochim. Acta Theriol. **103**: 104–120. doi:10.1016/j.gca.2012.10.037

McCarthy, M. D., R. Benner, C. Lee, and M. L. Fogel. 2007. Amino acid nitrogen isotopic fractionation patterns as indicators of heterotrophy in plankton, particulate, and dissolved organic matter. Geochim. Cosmochim. Acta **71**: 4727–4744. doi:https://doi.org/10.1016/j.gca.2007.06.061

McClelland, J. W., C. M. Holl, and J. P. Montoya. 2003. Relating low $\delta^{15}N$ values of zooplankton to N2-fixation in the tropical North Atlantic: Insights provided by stable isotope ratios of amino acids. Deep. Res. Part I Oceanogr. Res. Pap. **50**: 849–861. doi:10.1016/S0967-0637(03)00073-6

McCutchan, J. H., W. M. Lewis, C. Kendall, and C. C. McGrath. 2003. Erratum: Variation in trophic shift for stable isotope ratios of carbon, nitrogen, and sulfur. Oikos **111**: 416. doi:10.1111/j.0030-1299.2005.erratum_1.x

McClelland, J. W., and J. P. Montoya. 2002. Trophic Relationships and the Nitrogen Isotopic Composition of Amino Acids in Plankton. Ecology **83**: 2173–2180. doi:10.1890/0012-9658(2002)083[2173:TRATNI]2.0.CO;2

McMahon, K. W., and M. D. McCarthy. 2016. Embracing variability in amino acid $\delta^{15}N$ fractionation: Mechanisms, implications, and applications for trophic ecology. Ecosphere **7**: 1–26. doi:10.1002/ecs2.1511

McMahon, K. W., M. D. McCarthy, O. A. Sherwood, T. Larsen, and T. P. Guilderson. 2015. Millennial-scale plankton regime shifts in the subtropical North Pacific Ocean. Science **350**: 1530–1533. doi:10.1126/science.aaa9942

Melin, F. 2013. GMIS - MERIS Monthly climatology sea surface Chlorophyll-a concentration (9km) in mg m^-3. European Commission, Joint Research Centre (JRC) [Dataset]. PID: http://data.europa.eu/89h/a59f5362-a8af-4e85-b2e7-7052d244045e

Michaels, A. F., and M. W. Silver. 1988. Primary production, sinking fluxes and the microbial food web. Deep Sea Res. Part A, Oceanogr. Res. Pap. **35**: 473–490. doi:10.1016/0198-0149(88)90126-4

Mompeán, C., A. Bode, E. Gier, and M. D. McCarthy. 2016. Bulk vs. amino acid stable N isotope estimations of metabolic status and contributions of nitrogen fixation to size-fractionated zooplankton biomass in the subtropical N Atlantic. Deep. Res. Part I Oceanogr. Res. Pap. **114**: 137–148. doi:10.1016/j.dsr.2016.05.005

Ohkouchi, N., and others. 2017. Advances in the application of amino acid nitrogen isotopic analysis in ecological and biogeochemical studies. Org. Geochem. **113**: 150–174. doi:10.1016/j.orggeochem.2017.07.009

Pedrosa-Pàmies, R., M. H. Conte, J. C. Weber, and R. Johnson. 2018. Carbon cycling in the Sargasso Sea water column: Insights from lipid biomarkers in suspended particles. Prog. Oceanogr. **168**: 248–278. doi:10.1016/j.pocean.2018.08.005

Popp, B. N., E. A. Laws, R. R. Bidigare, J. E. Dore, K. L. Hanson, and S. G. Wakeham. 1998. Effect of phytoplankton cell geometry on carbon isotopic fractionation. Geochim. Cosmochim. Acta **62**: 69–77. doi:10.1016/S0016-7037(97)00333-5

Popp, B. N., B. S. Graham, R. J. Olson, C. C. S. Hannides, M. J. Lott, G. A. López-Ibarra, F. Galván-Magña, and B. Fry. 2007. Insight into the trophic ecology of yellowfin tuna, *Thunnes albacares*, from compound-specific nitrogen isotope analysis of proteinaceous amino acids, p. 173–190.*In* T. D. Dawson and R. T. W. Siegwolf [eds.], Stable isotopes as indicators of ecological change. San Diego, CA: Elsevier.

Prahl, F. G., G. Eglinton, E. D. S. Corner, S. C. M. O'Hara, and T. E. V. Forsberg. 1984. Changes in plant lipids during passage through the gut of Calanus. J. Mar. Biol. Assoc. U.K. **65**: 547–560. doi:10.1017/S0025315400030022

Romero-Romero, S., C. A. Ka'apu-Lyons, B. P. Umhau, C. R. Benitez-Nelson, C. C. S. Hannides, H. G. Close, J. C. Drazen, and B. N. Popp. 2020. Deep zooplankton rely on small particles when particle fluxes are low. Limnol. Oceanogr. Lett. **5**: 410–416. doi:10.1002/lol2.10163

Sargent, J. R., and S. Falk-Petersen. 1988. The lipid biochemistry of calanoid copepods. Hydrobiologia **167–168**: 101–114. doi:10.1007/BF00026297

Schnetzer, A., and D. K. Steinberg. 2002. Natural diets of vertically migrating zooplankton in the Sargasso Sea. Mar. Biol. **141**: 89–99. doi:10.1007/s00227-002-0815-8

Siegel, D. A., K. O. Buesseler, S. C. Doney, S. F. Sailley, M. J. Behrenfeld, and P. W. Boyd. 2014. Global assessment of ocean carbon export by combining satellite observations and food-web models. Global Biogeochem. Cycles **28**: 181–196. doi:10.1002/2013GB004743

Sigman, D., K. Karsh, and K. Casciotti. 2009. Ocean process tracers: Nitrogen isotopes in the ocean, p. 4138–4153.*In* J. Steele, K. Turekian, and S. Thorpe [eds.], Encyclopedia of ocean sciences. London: Academic Press.

Stamieszkin, K., D. K. Steinberg, and A. E. Maas. 2021. Fecal pellet production by mesozooplankton in the subarctic Northeast Pacific Ocean. Limnol. Oceanogr. **9999**: 1–13. doi:10.1002/lno.11774

Steinberg, D. K., and M. R. Landry. 2017. Zooplankton and the ocean carbon cycle. Ann. Rev. Mar. Sci. **9**: 413–444. doi:10.1146/annurev-marine-010814-015924

Tamelander, T., J. E. Søreide, H. Hop, and M. L. Carroll. 2006. Fractionation of stable isotopes in the Arctic marine copepod *Calanus glacialis*: Effects on the isotopic composition of marine particulate organic matter. J. Exp. Mar. Bio. Ecol. **333**: 231–240. doi:10.1016/j.jembe.2006.01.001

Turner, J. T. 2002. Zooplankton fecal pellets, marine snow and sinking phytoplankton blooms. Aquat. Microb. Ecol. **27**: 57–102. doi:10.3354/Ame027057

Turner, J. T. 2015. Zooplankton fecal pellets, marine snow, phytodetritus and the ocean's biological pump. Prog. Oceanogr. **130**: 205–248. doi:10.1016/j.pocean.2014.08.005

Vokhshoori, N. L., T. Larsen, and M. D. McCarthy. 2014. Reconstructing δ13C isoscapes of phytoplankton production in a coastal upwelling system with amino acid isotope values of littoral mussels. Mar. Ecol. Prog. Ser. **504**: 59–72. doi:10.3354/meps10746

Wakeham, S. G., and E. A. Canuel. 1988. Organic geochemistry of particulate matter in the eastern tropical North Pacific Ocean: Implications for particle dynamics. J. Mar. Res. **46**: 183–213. doi:10.1357/002224088785113748

Wall, C. B., N. J. Wallsgrove, R. D. Gates, and B. N. Popp. 2021. Amino acid $\delta^{13}C$ and $\delta^{15}N$ analyses reveal distinct species-specific patterns of trophic plasticity in a marine symbiosis. Limnol. Oceanogr. **9999**: 1–18. doi:10.1002/lno.11742

Wexels Riser, C., P. Wassmann, M. Reigstad, and L. Seuthe. 2008. Vertical flux regulation by zooplankton in the northern Barents Sea during Arctic spring. Deep-Sea Research II **55**: 2320–2329. doi:10.1016/j.dsr2.2008.05.006

Yamaguchi, Y. T., and M. D. McCarthy. 2018. Sources and transformation of dissolved and particulate organic nitrogen in the North Pacific Subtropical Gyre indicated by compound-specific δ15N analysis of amino acids. Geochim. Cosmochim. Acta **220**: 329–347. doi:https://doi.org/10.1016/j.gca.2017.07.036

Yamaguchi, Y. T., Y. Chikaraishi, Y. Takano, N. O. Ogawa, H. Imachi, Y. Yokoyama, and N. Ohkouchi. 2017. Fractionation of nitrogen isotopes during amino acid metabolism in heterotrophic and chemolithoautotrophic microbes across eukarya, bacteria, and archaea: Effects of nitrogen sources and metabolic pathways. Org. Geochem. **111**: 101–112. doi:10.1016/j.orggeochem.2017.04.004

Acknowledgments

Thank you to the crew and science parties of the cruises LMG 1801, RR1813, AE 1819, and AE 1910 for helping collect zooplankton and produce fecal pellet samples, particularly Joe Cope, Patricia Thibodeau, Andrea Miccoli, and Karen Stamieszkin—who also advised us on experimental container design. This work was made possible by funding from: NSF OCE 1830016 to H.G.C., NSF OCE 1829318 to A.E.M., BIOS-SCOPE funding from Simons Foundation International to A.E.M. and H.G.C., NASA-80NSSC17K0654 to D.K.S. and A.E.M., NSF PLR 1440435 (Antarctic Organisms and Ecosystems Program) to D.K.S., NSF PLR 1643345 and NSF OCE 1829425 to B.N.P. We are grateful to Albert Ortiz, Joshua Pi, and Suzanne Stremler for assistance with laboratory analysis and to Lillian Henderson for assistance with chlorophyll data, and we thank two anonymous reviewers for their thoughtful comments. Data from the paper will be published at the BCO-DMO online database: EXPORTS project data can be found at https://www.bco-dmo.org/project/768320 and BIOS-SCOPE project data can be found at https://www.bco-dmo.org/project/826178. Palmer LTER core data can be found at https://pal.lternet.edu/data. This is SOEST contribution number 11330 and contribution 4014 of the Virginia Institute of Marine Science, William & Mary.

Conflict of Interest

There were no conflicts of interest from the authors or any funding sources to this work.

Submitted 04 September 2020
Revised 17 February 2021
Accepted 25 April 2021

Associate editor: Thomas Kiørboe